Anal. Chem. **2007,** *79,* 6927−6932

Lactate and Sequential Lactate−Glucose Sensing Using Surface-Enhanced Raman Spectroscopy

Nilam C. Shah,† Olga Lyandres,‡ Joseph T. Walsh, Jr.,‡ Matthew R. Glucksberg,‡ and Richard P. Van Duyne*,†

Chemistry Department and Department of Biomedical Engineering, Northwestern University, Evanston, Illinois 60208

Lactate production under anaerobic conditions is indicative of human performance levels, fatigue, and hydration. Elevated lactate levels result from several medical conditions including congestive heart failure, hypoxia, and diabetic ketoacidosis. Real-time detection of lactate can therefore be useful for monitoring these medical conditions, posttrauma situations, and in evaluating the physical condition of a person engaged in strenuous activity. This paper represents a proof-of-concept demonstration of a lactate sensor based on surface-enhanced Raman spectroscopy (SERS). Furthermore, it points the direction toward a multianalyte sensing platform. A mixed decanethiol/mercaptohexanol partition layer is used herein to demonstrate SERS lactate sensing. The reversibility of the sensor surface is characterized by exposing it alternately to aqueous lactate solutions and buffer without lactate. The partitioning and departitioning time constants were both found to be ∼30 s. In addition, physiological lactate levels (i.e., 6−240 mg/dL) were quantified in phosphate-buffered saline medium using multivariate analysis with a root-mean-square error of prediction of 39.6 mg/dL. Finally, reversibility was tested for sequential glucose and lactate exposures. Complete partitioning and departitioning of both analytes was demonstrated.

Elevated blood lactate concentration is a predictor of a number of medical conditions[1] including the survival of children in open heart surgery,[2] mortality in ventilated infants,[3] death as a result of septic shock in adults,[4] decreased tissue oxidation, hypovolemic left heart failure, and drug toxicity.[5] Blood lactate is also a valuable indicator for clinical diagnosis, exercise, and athletic performance.[5−13] There are several studies that indicate the therapeutic importance of maintaining normal blood lactate levels in critically ill patients.[14−18] For example, Smith and co-workers showed that intensive care patients whose blood lactate levels were normalized in the first 24 h had a mortality rate of 24% while the inability to normalize lactate levels within 24 h resulted in 82% mortality rate.[17] It is clear from these studies that monitoring lactate in real time has significant implications in many clinical situations.

Currently, the most common clinical method to measure lactate involves collecting a blood sample and analyzing the sample by enzyme-mediated electrochemical methods.[19−21] Handheld lactate sensors, analogous to those for glucose, are also available at modest cost.[22] However, this method is painful, indirect, and only reports on lactate concentrations at discrete intervals when blood is drawn. Therefore, developing a sensor that can measure lactate levels directly and in real time would be a valuable addition to the techniques available for metabolic monitoring. Surface-enhanced Raman spectroscopy (SERS) offers a new approach to real-time monitoring of lactate by directly measuring the vibrational spectrum of molecules within ∼2 nm of the SERS-active surface.

In addition, generalizing this SERS sensor for multianalyte detection will be useful in metabolic monitoring and diagnosing a wide variety of diseases.[23] For example, monitoring both glucose and lactate can help determine if a patient is suffering from

* To whom correspondence should be addressed. E-mail: vanduyne@northwestern.edu. Fax: 847-491-7713.

† Chemistry Department.

‡ Department of Biomedical Engineering.

(1) Burtis, C.; Ashwood, E. R. *Tietz Textbook of Clinical Chemistry*; Saunders: London, 1999.
(2) Siegel, L. B.; Dalton, H. J.; Hertzog, J. H.; Hopkins, R. A.; Hannan, R. L.; Hauser, G. J. *Intensive Care Med.* **1996**, *22*, 1418−1423.
(3) Deshpande, S. A.; Platt, M. P. *Archi. Dis. Childhood. Fetal Neonat. Ed.* **1997**, *76*, F15−F20.
(4) Bakker, J.; Gris, P.; Coffernils, M.; Kahn, R. J.; Vincent, J. L. *Am. J. Surg* **1996**, *171*, 221−226.
(5) Palleschi, G.; Mascini, M.; Bernardi, L.; Zeppilli, P. *Med. Biol. Eng. Comput.* **1990**, *28*, B25−B28.
(6) D'Auria, S.; Gryczynski, Z.; Gryczynski, I.; Rossi, M.; Lakowicz, J. R. *Anal. Biochem.* **2000**, *283*, 83−88.
(7) Liu, X.; Tan, W. *Mikrochim. Acta* **1999**, *131*, 129−135.
(8) Hirano, K.; Yamato, H.; Kunimoto, K.; Ohwa, M. *Biosens. Bioelectron.* **2002**, *17*, 315−322.
(9) Nakamura, H.; Karube, I. *Anal. Bioanal. Chem.* **2003**, *377*, 446−468.
(10) Moser, I.; Jobst, G.; Urban, G. A. *Biosens. Bioelectron.* **2002**, *17*, 297−302.
(11) Baker, D. A.; Gough, D. A. *Anal. Chem.* **1995**, *67*, 1536−1540.
(12) Yang, L.; Kissinger, P. T. *Curr. Sep.* **1995**, *14*, 31−35.
(13) Jobst, G.; Moser, I.; Varahram, M.; Svasek, P. E. A.; Trajanoski, Z.; Wach, P.; Kotanko, P.; Skraba, F.; Urban, G. *Anal. Chem.* **1996**, *68*, 3173−3179.
(14) Bakker, J.; Pinto de Lima, A. *Crit. Care* **2004**, *8*, 96−98.
(15) Meregalli, A.; Oliveira, R. P.; Friedman, G. *Crit. Care* **2004**, *8*, R60−R65.
(16) Waxman, K.; Nolan, L. S.; Shoemaker, W. C. *Crit. Care Med.* **1982**, *10*, 96−99.
(17) Smith, I.; Kumar, P.; Molloy, S.; Rhodes, A.; Newman, P. J.; Grounds, R. M.; Bennet, E. D. *Intensive Care Med.* **2001**, *27*, 74−83.
(18) Blow, O.; Magliore, L.; Claridge, J. A.; Butler, K.; Young, J. S. *J. Trauma* **1999**, *47*, 964−969.
(19) Fox, E. L.; Bowers, R. W.; Foss, M. L. *The physiological basis of physical education and athletics*; Brown and Benchmark Publishers: Madison, WI, 1989.
(20) McArdle, W. D.; Katch, F. I.; Katch, V. L. *Exercise Physiology: Energy, Nutrition and Human Performance*; Lea and Febiger: Philadelphia, 1991.
(21) Billat, L. V. *Sports Med.* **1996**, 157−175.
(22) Accusport: http://www.lactate.com, 2007.
(23) Kurita, R.; Hayashi, K.; Fan, X.; Yamamoto, K.; Kato, T.; Niwa, O. *Sens. Actuators, B: Chem.* **2002**, *87*, 296−303.

10.1021/ac0704107 CCC: $37.00
Published on Web 08/10/2007

ischemia. During ischemia, there is inadequate blood flow to a particular region of the body and therefore less oxygenation of the tissue. If anaerobic conditions exist, glucose will be metabolized to lactate, resulting in an increase in lactate concentration and decrease in glucose concentration.[23] Simultaneous lactate and glucose measurements are also useful for understanding diabetes where there is a rise in lactate levels following hypoglycemia.[24]

There are several other indirect techniques being developed for lactate sensing including the use of holographic sensors and sol−gel encapsulation for optical sensing of lactate.[25,26] However, these techniques have limitations including indirect measurement, selectivity, and sensitivity.

Raman spectroscopy, on the other hand, detects molecules directly, and the potential of Raman spectroscopy for lactate detection has already been demonstrated.[27−29] However, although results are promising, Raman spectroscopy is not able to detect the requisite low physiological levels of lactate (i.e., 6−240 mg/dL).[27] The effective Raman cross section can be amplified for visible and NIR excitation wavelengths with SERS.[30,31] Using SERS retains all of the advantages of normal Raman spectroscopy while achieving significantly higher sensitivity. SERS has not been widely used for biological analysis due to concerns about nonspecific protein adsorption and surface degradation. To combat these problems, we have developed a technique that utilizes a highly reproducible SERS-active substrate functionalized with a self-assembled monolayer (SAM), which preconcentrates the analyte within the 0−2-nm detection zone of SERS thus preventing fouling and improving the specificity of the sensor.[32]

In our previous work on glucose sensing with SERS, we increased the glucose concentration within the detection zone of SERS by using a SAM on a silver film-over-nanospheres (AgFON) substrate.[33−36] The SAM function is analogous to the stationary phase in high-performance liquid chromatography.[37−41] Among various SAMs tested,[33,34] a mixed monolayer consisting of decanethiol (DT) and mercaptohexanol (MH) has been shown to have optimal performance for partitioning and departitioning glucose.[36] We have demonstrated the stability and reversibility of the dual DT/MH SAM and quantitative detection of glucose using the SAM-functionalized SERS sensor. Furthermore, we have shown that in vivo SERS detection is feasible by testing the glucose SERS sensor in the rat animal model.[42] Due to the success of this SAM in detecting glucose, we used the DT/MH-functionalized AgFON as an initial sensing platform for lactate detection. However, since the DT/MH SAM will exhibit different interactions with different analytes, a careful examination of lactate partitioning into the SAM is required to demonstrate the feasibility of lactate sensing with SERS.

The work presented in this study demonstrates the proof of concept for the development of the first SERS lactate biosensor. Furthermore, we present preliminary data toward the development of the first general multianalyte platform based on SERS. We successfully show the following: (1) reversibility of the SERS sensor for lactate using the DT/MH SAM; (2) quantitative measurement of lactate; (3) rapid partitioning/departitioning time constants following a step change in concentration; and (4) detection of multiple analytes (i.e., glucose and lactate) with the DT/MH-functionalized sensing platform.

EXPERIMENTAL SECTION

Materials. All the chemicals were reagent grade or better and used as purchased. Silver pellets (99.99%) were purchased from Kurt J. Lesker Co. (Clairton, PA). Titanium was obtained from McMaster-Carr (Chicago, IL) and cut into 18-mm-diameter disks. To clean the Ti substrates, 95.5−96.5% H_2SO_4 was purchased from EMD Chemicals, NH_4OH, and H_2O_2 were from Fisher Scientific (Fairlawn, VA). Surfactant-free, white carboxyl-substituted latex polystyrene nanosphere suspensions (390 ± 19.5-nm diameter, 4% solid) were purchased from Duke Scientific Corp. (Palo Alto, CA). Ultrapure water (18.2 MΩ cm^{-1}) from a Millipore system (Marlborough, MA) was used for substrate and solution preparation. Glucose and lactate were purchased from Sigma (St. Louis, MO). Ethanol was purchased from Fisher Scientific (Fairlawn, VA). Decanethiol, and 6-mercapto-1-hexanol were purchased from Aldrich (Milwaukee, WI).

AgFON Fabrication and Incubation Procedure. The titanium substrates were cleaned by placing them in a 4:1 solution of H_2SO_4/H_2O for several minutes. The substrates were then placed in a 5:1:1 solution of H_2O/30% H_2O_2/NH_4OH and sonicated. Approximately 10 μL of nanosphere solution was drop-coated onto a clean titanium substrate and allowed to dry at room temperature. Then, 200-nm-thick Ag films were deposited onto and through the nanosphere mask using the Kurt J. Lesker electron beam deposition system (Clairton, PA) to form AgFON substrates. The mass thickness and deposition rate (1 Å/s) of the Ag metal were measured by a 6-MHz gold-plated quartz crystal microbalance purchased from Sigma Instruments (Fort Collins, CO). AgFON substrates were first incubated in 1 mM DT in ethanol for 45 min and then transferred to 1 mM MH in ethanol for at least 12 h.

(24) Maran, A.; Cranston, I. J. L.; Macdonald, I.; Amiel, S. A. *Lancet* **1994**, *343*, 16−20.
(25) Sartain, F. K.; Yang, X.; Lowe, C. *Anal. Chem.* **2006**, *78*, 5664−5670.
(26) Li, C. I.; Lin, Y. H.; Shih, C. L.; Tsaur, J. P.; Chau, L. K. *Biosens. Bioelectron.* **2002**, *17*, 323−330.
(27) Pilotto, S.; Pacheco, M. T. T.; Silveira, L., Jr.; Balbin Villaverde, A.; Zangaro, R. A. *Lasers Med. Sci.* **2001**, *16*, 2−9.
(28) Erckens, R. J.; Motamedi, M.; March, W. F.; Wicksted, J. P. *J. Raman Spectrosc.* **1997**, *28*, 293−299.
(29) Berger, A. J.; Wang, Y.; Feld, M. S. *Appl. Opt.* **1996**, *35*, 209−212.
(30) Yonzon, C. R.; Lyandres, O.; Shah, N. C.; Dieringer, J. A.; Van Duyne, R. P. In *Surface-Enhanced Raman Scattering: Physics and Applications*; Kneipp, K., Moskovits, M., Kneipp, H., Eds.; Spinger-Verlag: Berlin, 2006; Vol. 103, pp 367−379.
(31) Haynes, C. L.; McFarland, A. D.; Van Duyne, R. P. *Anal. Chem.* **2005**, *77*, 338A−346A.
(32) Dieringer, J. A.; McFarland, A. D.; Shah, N. C.; Stuart, D. A.; Whitney, A. V.; Yonzon, C. R.; Young, M. A.; Yuen, J.; Zhang, X.; Van Duyne, R. P. *Faraday Discuss.* **2006**, *132*, 9−26.
(33) Shafer-Peltier, K. E.; Haynes, C. L.; Glucksberg, M. R.; Van Duyne, R. P. *J. Am. Chem. Soc.* **2003**, *125*, 588−593.
(34) Yonzon, C. R.; Haynes, C. L.; Zhang, X. Y.; Walsh, J. T.; Van Duyne, R. P. *Anal. Chem.* **2004**, *76*, 78−85.
(35) Stuart, D. A.; Yonzon, C. R.; Zhang, X.; Lyandres, O.; Shah, N. C.; Glucksberg, M. R.; Walsh, J. T.; Van Duyne, R. P. *Anal. Chem.* **2005**, *77*, 4013−4019.
(36) Lyandres, O.; Shah, N. C.; Yonzon, C. R.; Walsh, J. T., Jr.; Glucksberg, M. R.; VanDuyne, R. P. *Anal. Chem.* **2005**, *77*, 6134−6139.
(37) Freunscht, P.; Van Duyne, R. P.; Schneider, S. *Chem. Phys. Lett.* **1997**, *281*, 372−378.
(38) Blanco Gomis, D.; Muro Tamayo, J.; Alonso, M. *Anal. Chim. Acta* **2001**, *436*, 173.
(39) Yang, L.; Janle, E.; Huang, T.; Gitzen, J.; Kissinger, P. T.; Vreeke, M.; Heller, A. *Anal. Chem.* **1995**, *34*, 1326−1331.
(40) Carron, K. T.; Kennedy, B. J. *Anal. Chem.* **1995**, *67*, 3353−3356.
(41) Deschaines, T. O.; Carron, K. T. *Appl. Spectrosc.* **1997**, *51*, 1355−1359.
(42) Stuart, D. A.; Yuen, J. M.; Lyandres, N. S. O.; Yonzon, C. R.; Glucksberg, M. R.; Walsh, J. T.; Van Duyne, R. P. *Anal. Chem.* **2006**, *78*, 7211−7215.

Then the SAM-functionalized surfaces were mounted into a small-volume flow cell for SER spectra collection.

Surface-Enhanced Raman Spectroscopy. A Spectra-Physics model Millennia Vs laser was used to produce the 532-nm excitation wavelength (λ_{ex}); the laser spot size on the sample was usually 100 μm in diameter. This excitation wavelength was chosen to produce high signal-to-noise spectra for our initial demonstration of the direct detection of lactate. The SERS-active substrates used in these studies (sphere mask diameter, D = 390 nm) provide optimal enhancement when used with 532-nm excitation wavelength.[43,44] Furthermore, Raman scattering intensity is inversely proportional to λ,[4] resulting in a 1.5 times stronger signal at shorter wavelengths (e.g., 532 nm). NIR excitation wavelength (e.g., 785 nm) would be more appropriate in the studies involving complex biological environments or in vivo models to reduce the fluorscence background and increase penetration depth. Although the Raman intensity will decrease with the use of 785-nm excitation, the structure of the SERS-active surface can be optimized to match the excitation wavelength in order to maintain the enhancements needed for detecting lactate. The SERS measurement system includes an interference filter, an edge filter (Semrock, Rochester, NY), a model VM-505 single-grating monochromator with the entrance slit set at 100 μm (Acton Research Corp., Acton, MA), and a LN_2-cooled CCD detector (Roper Scientific, Trenton, NJ). A collection lens with magnification 5 was used to collect the scattered light. The small-volume flow cell was used to control the external environment of the AgFON surfaces throughout the SERS experiments. In all experiments, the flow cell was filled by manual injection with the test solution. It remained static in the flow cell during Raman data acquisition.

Quantitative Multivariate Analysis. All data processing was performed using MATLAB (MathWorks, Inc., Natick, MA) and PLS_Toolbox (Eigenvector Research, Inc., Manson, WA). Prior to analysis, the spectra were smoothed using the Savitsky−Golay method with a second-order polynomial and window size of 9. Cosmic rays were removed from the spectra using a derivative filter. The slowly varying background, commonly seen in SERS experiments, was removed by subtracting a fourth-order polynomial fit. This method greatly reduced varying background levels with minimum effect on the SERS peaks. The chemometric analysis was performed using the partial least-squares (PLS) method and leave-one-out (LOO) cross-validation algorithm.

Time Constant Analysis. The data were processed using PeakFit 4.12 software (Systat Software Inc, Richmond, CA). To remove the varying background in SER spectra, a fourth-order polynomial was subtracted from the baseline using MATLAB software. The spectra were further preprocessed in PeakFit with linear best-fit baseline correction and Savitsky−Golay smoothing. The amplitude of the Raman bands was obtained by fitting the data with a superposition of the Lorentzian amplitude line shapes.

RESULTS AND DISCUSSION

Reversibility of Lactate Sensor. To demonstrate the reversibility of the SERS lactate sensor, the DT/MH-modified AgFON surface was exposed to cycles of 0 and 100 mM aqueous lactate solutions (pH ~5) without flushing the sensor in between measurements in order to simulate real-time sensing (Figure 1 inset). Traces A−D in Figure 1 show the SER spectra collected for each step change in concentration. The total data acquisition time, t_{acq}, for each step was 20 min (λ_{ex} = 532 nm, P = 10 mW, t_{acq} = 20 min). The emergence and disappearance of the lactate band at 868 cm^{-1} should be noted as the lactate concentration is cycled. Due to spectral overlap between the SER spectrum of the SAM and lactate, we compute the difference spectra to visually demonstrate the lactate signal. Figure 1E shows the normal Raman spectrum of a 0.8 M aqueous lactate solution as a reference. In the normal Raman spectrum of lactate, peaks at 1457, 1420, 1368, 1321, 1276, 1127, 1090, 1048, 934, and 866 cm^{-1} correspond to aqueous lactate ion peaks.[45] The difference spectra (Figure 1F, G) represent partitioning of lactate in DT/MH SAM, which clearly exhibit the lactate bands at 1463, 1422, 1272, 1134, 1094, 1051, 936, and 868 cm^{-1}. Slight differences in peak position between normal Raman and SERS are commonly observed due to interaction of the molecule with the partition layer and the metal surface. Comparing the SER spectrum of the SAM before injecting lactate (Figure 1A) and after rinsing and departitioning of lactate (Figure 1C), no trace of lactate remains. The absence of lactate spectral features in the difference spectra (Figure 1H) shows the complete departitioning of lactate. Moreover, the difference between the two spectra in which lactate is present at identical concentrations (Figure 1B, D) reveal no change in the measured signal intensity (Figure 1I). Although quantitative data can be obtained in t_{acq} = 2 min (see below), longer acquisition times have been used to obtain the difference spectra with a high signal-to-

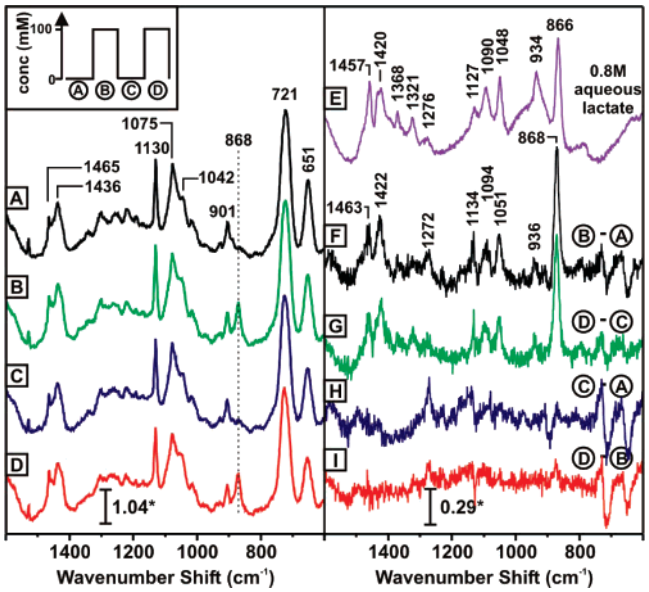

Figure 1. Inset: step changes in lactate concentration experienced by the sensor. (A−D) SER spectra collected for each step. (E) Normal Raman spectrum of 0.8 M aqueous lactate solution. (F−I) show the differences indicating lactate partitioning and departitioning. Raman bands in the difference spectra showing lactate (F, G) agree well with the reference lactate spectrum (E). *denotes analog-to-digital units mW^{-1} s^{-1}. λ_{ex} = 532 nm, P = 10 mW, and t_{acq} = 20 min.

(43) McFarland, A. D.; Young, M. A.; Dieringer, J. A.; Van Duyne, R. P. *J. Phys. Chem. B* **2005**, *109*, 11279−11285.
(44) Zhang, X.; Young, M. A.; Lyandres, O.; Van Duyne, R. P. *J. Am. Chem. Soc.* **2005**, *127*, 4484−4489.
(45) Cassanas, G.; Morssli, M.; Fabregue, E.; Bardet, L. *J. Raman Spectrosc.* **1991**, *22*, 409−413.

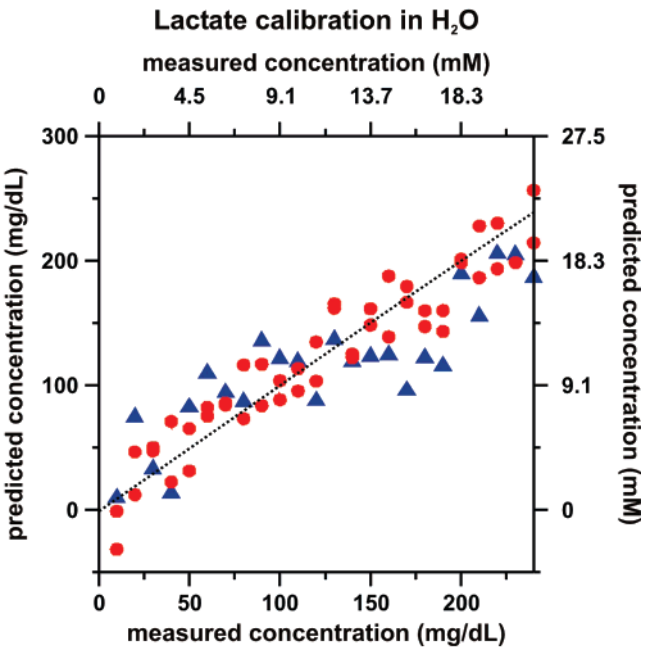

Figure 2. Lactate calibration (circles) and validation (triangles) plot using multiple spots on a single substrate in water. The PLS calibration plot was constructed using 48 data points, and the validation plot was constructed using 24 data points taken over a range of lactate concentrations (10−240 mg/dL). RMSEC = 21.64 mg/dL (2 mM) and RMSEP = 37.58 mg/dL (3.4 mM) with 7 loading vectors. λ_{ex} = 532 nm, P = 7−12 mW, and t_{acq} = 2 min.

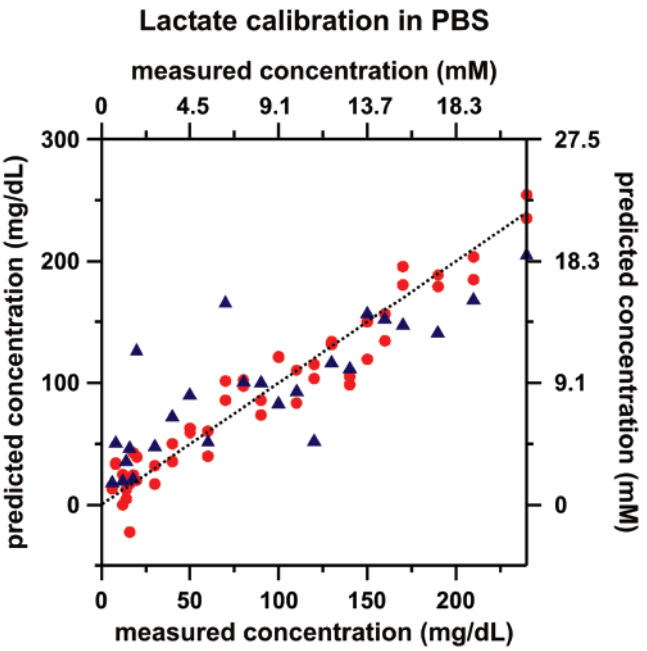

Figure 3. Lactate calibration (circles) and validation (triangles) plot using multiple spots on a single substrate in PBS. The PLS calibration plot was constructed using 50 data points, and the validation plot was constructed using 25 data points taken over a range of lactate concentrations (6−240 mg/dL). RMSEC = 17.8 mg/dL (1.6 mM) and RMSEP = 39.6 mg/dL (3.6 mM) with 7 loading vectors. λ_{ex} = 532 nm, P = 7−12 mW, and t_{acq} = 2 min.

noise ratio. These data clearly demonstrate that the DT/MH mixed SAM is a completely reversible sensing surface for optimal partitioning and departitioning of lactate.

Quantitative Lactate Detection. We demonstrate quantitative lactate detection in the clinically relevant range 6−240 mg/dL (0.5−22 mM) in a simple aqueous system and in a system buffered with phosphate buffered-saline (PBS) (Figure 2, Figure 3). DT/MH-functionalized AgFON samples were placed in a flow cell, and lactate solutions ranging from 6 to 240 mg/dL were randomly introduced into the cell and incubated for 2 min to ensure complete partitioning. SER spectra were collected at multiple locations on the surface with a visible laser source, with an integration time of 2 min for each spectrum (λ_{ex} = 532 nm, P = 7.5−12 mW, t_{acq} = 2 min). Calibration models were constructed using partial least-squares leave-one-out (PLS-LOO) analysis with 48−50 randomly chosen independent spectral measurements of known lactate concentrations. The calibration models were based upon seven latent variables that take into account variation in laser power, the environment in the laboratory, and SERS enhancement at different locations. The PLS analysis results in a root-mean-square error of calibration (RMSEC) of 21.64 mg/dL (2 mM) for the water system and 17.8 mg/dL (1.6 mM) for the buffered system.

For validation of the models, sets of 24−25 independent data points were used. The root-mean-square error of prediction (RMSEP) was calculated to be 37.58 mg/dL (3.4 mM) for the aqueous system and 39.6 mg/dL (3.6 mM) for the PBS system. These data reflect an initial attempt to quantify lactate concentrations in the physiological range using SERS. The data demonstrate the feasibility of lactate measurements, but also make apparent the need for further optimization of the sensing platform to improve the detection limits and reduce prediction errors. The RMSEP can be improved by increasing the number of data points in the calibration set. However, the main feature that controls the sensitivity and selectivity of the sensor is the partition layer on the SERS-active surface. This can be further optimized to improve sensing performance.

Real-Time Partitioning and Departitioning of Lactate. In addition to reversibility, an important characteristic for a viable sensor, the sensor should be able to partition and departition the analyte of interest on a reasonable time scale. The real-time response for lactate was examined in an aqueous system. To evaluate the real-time response of the sensor, the $1/e$ time constant for partitioning and departitioning was obtained using a DT/MH-functionalized AgFON mounted in a flow cell in an aqueous solution. SER spectra were collected continuously for 10 min with 15-s integration time for each frame at an excitation wavelength of 532 nm. To observe partitioning, 100 mM aqueous lactate solution was rapidly injected at t = 0. At t = 315 s, 0 mM lactate solution was rapidly injected into the flow cell to observe departitioning. The partitioning dynamics of lactate were evaluated by examining the intensity of the C—COO^- vibrational stretch of lactate at 860 cm^{-1}.[45] The time constant was determined by fitting an exponential curve to the data as shown in Figure 4. The estimated $1/e$ time constant for partitioning and departitioning of lactate was less than 30 s. The uncertainty in the time constant of several seconds is attributed to delays in concentration step changes and smoothing of the data by the 15-s integration time. This response time indicates that the DT/MH-functionalized AgFON sensor is capable of detecting lactate quickly, which is important in critical care situations.

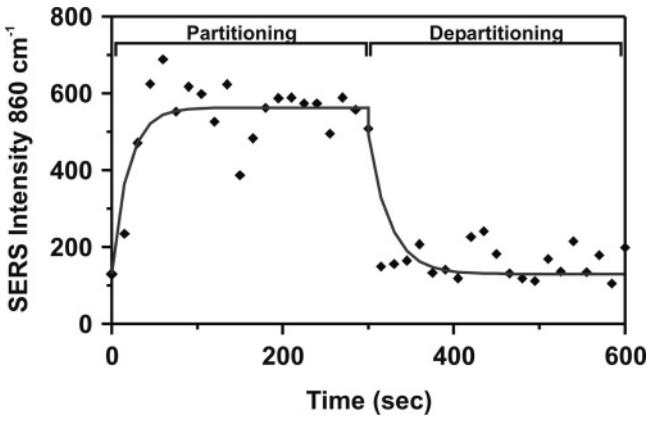

Figure 4. Real-time SERS response to a step change in lactate concentration in water. The 100 mM lactate was injected at $t = 0$ s, and the cell was flushed with water at $t = 315$ s. $\lambda_{ex} = 532$ nm, $P_{laser} = 10.6$ mW, and $t_{acq} = 15$ s. The $1/e$ time constants were calculated to be less than 30 s for partitioning and departitioning.

Sequential Lactate/Glucose Sensing. In an effort to generalize the SERS sensing platform and develop a device for rapid detection of multiple analytes in a clinical setting, we demonstrate that we can utilize the same SAM-functionalized AgFON surface to sequentially detect both lactate and glucose. The experiment was conducted by alternatively injecting 100 mM glucose and 100 mM lactate solutions into the flow cell and rinsing the surface with PBS between each step, with a total acquisition time of 20 min for each spectrum (Figure 5A). Similar to the results above for reversibility of lactate, difference spectroscopy is utilized to analyze the data since the SAM itself has a Raman signature. For example, to obtain a spectrum of glucose, we perform a subtraction: step 2 (SAM + PBS + glucose) minus step 1 (SAM + PBS). Figure 5B depicts the mean spectrum of glucose obtained by averaging both glucose difference spectra (steps 2 − 1 and steps 6 − 5). The prominent glucose bands at 915, 1073, 1126, 1268, 1373, and 1462 cm^{-1} match the peaks in a reference glucose spectrum.[46] Similarly, Figure 5C demonstrates the mean difference spectrum of lactate (steps 4 − 3 and steps 8 − 7) with bands at 866, 934, 1048, 1090, 1127, 1321, 1420, and 1457 cm^{-1} matching the lactate Raman signature.[45] The results indicate that both analytes (glucose and lactate) partition and departition successfully from the SAM and the difference spectra of both analytes (Figure 5) match well with previously published spectra of glucose and lactate. Finally, when the surface is rinsed with PBS, the results indicate that both glucose and lactate departition completely. Specifically, Figure 5D shows a representative difference spectrum of subsequent rinsing steps (steps 3 − 1) that has no residual peaks from glucose. While there are no glucose bands, the subtraction does not produce a completely flat spectrum due to minor rearrangements of the SAM throughout the experiment. Similarly, a difference spectrum between lactate injections (i.e., steps 5 − 3) does not contain any lactate Raman bands, indicating complete departitioning of lactate (data not shown). Therefore, we can conclude that the interactions are reversible and the sensor can be used to track fluctuations in concentration levels of glucose and lactate. This is the first step toward the development of a general sensing platform for rapid detection of multiple bioanalytes.

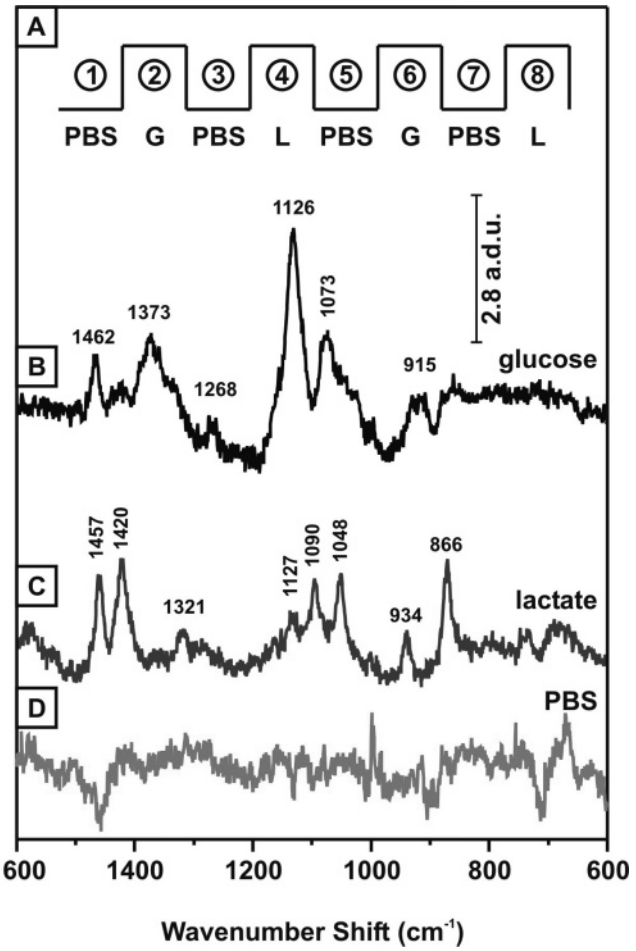

Figure 5. (A) Step changes of glucose (G) and lactate (L) concentrations (0−100 mM) introduced into the sensor with PBS rinsing between the introduction of each analyte. (B) Mean difference spectrum (average of difference between steps 2 − 1 and 6 − 5) demonstrating partitioning of glucose. (C) Mean difference spectrum (average of difference between steps 4 − 3 and 8 − 7) demonstrating partitioning of lactate. (D) representative difference spectrum of consecutive rinsing steps (3 − 1) demonstrating departitioning of glucose since the difference spectrum returns to baseline. *denotes analog-to-digital units $mW^{-1}s^{-1}$. $\lambda_{ex} = 532$ nm, $P = 13$ mW, and $t_{acq} = 10$ min.

CONCLUSIONS

This work demonstrates the first application of SERS for the development of a lactate sensor and a multianalyte sensing platform. The reversibility of the DT/MH-functionalized SERS surface for lactate has been demonstrated. The DT/MH-functionalized SERS surface partitioned and departitioned lactate in ∼30 s, indicating that the sensor response is rapid enough for real-time, continuous sensing. In addition, quantitative lactate measurements in the physiological concentration range (6−240 mg/dL) in water and in PBS were also demonstrated. Finally, the reversibility of the DT/MH-functionalized SERS surface for both glucose and lactate was also demonstrated.

In future work, different partition layers and fabrication methods will be explored to minimize spectral overlap and achieve

(46) Soderholm, S.; Roos, Y. H.; Meinander, N.; Hotokka, M. *J. Raman Spectrosc.* **1999**, *30*, 1009−1018.

optimal lactate and multiple analyte sensing. Furthermore, the sensor response will be examined with sequential and simultaneous exposure to glucose and lactate at varying concentrations to quantify signal changes due to fluctuations of analyte concentrations and competing affinity of analytes to the SAM. A detailed study of the simultaneous detection of glucose and lactate on the multisensing platform will be reported in a future publication. Once optimal conditions are achieved, we will implant the sensor in an animal model to demonstrate continuous in vivo sensing.

ACKNOWLEDGMENT

This work was supported by the National Institutes of Health (DK066990-01A1), the U.S. Army Medical Research and Material Command (W81XWH-04-1-0630), the National Science Foundation (CHE0414554), and the Air Force Office of Scientific Research MURI program (F49620-02-1-0381).

Received for review February 27, 2007. Accepted June 29, 2007.

AC0704107